Compression modeling in the large square baler

Kenny Nona, Erdal Kayacan, Wouter Saeys, University of Leuven (KU Leuven), Department of Biosystems (BIOSYST), Division of Mechatronics, Biostatistics and Sensors (MeBioS), Leuven, Belgium

Abstract

The compression of biological materials is essential for facilitating their transport and storage. Large square balers are often used for this purpose as they can operate continuously and thus can reach high capacities. However, the high compression forces lead to a high energy consumption. To optimize the energy consumption, a mathematical model describing the impact of the machine settings and design parameters on the compression process is required. Such a model is elaborated in this paper by deriving the static momentum equations to describe forces and deformations along the compression chamber. To describe the compression characteristics of the material, a linear elastic model with isotropic material parameters is implemented. This model is then applied to estimate the material properties of the crop in the bale chamber by minimizing the squared difference between the predicted and measured deformation along the bale chamber.

1. Introduction

Biological materials such as wheat straw and silage, are transported from the field to the farm or the factory. For reducing transport and storage costs, the biological materials are compressed. Extrusion is preferred over fixed wall compression as it allows continuous operation. For this purpose, large square balers are widely used as high capacities can be reached with these machines. However, these machines have a high power requirement, leading to a high energy consumption. To better control these machines and reduce the energy consumption, a mathematical description of the compression process in a compression chamber with inclined walls is needed.

Ferrero et al. modeled the decay of the compression force along a compression box with constant cross section [1]. In extrusion, the cross section becomes smaller towards the exit of the chamber which makes this model not applicable for extruders. Also they were not able to calculate the deformation along the length of the compression box, while this is an essential performance parameter. Faborode & O'Callaghan modeled the pressure in a compression box as a function of the crop parameters and plunger position [2]. However, they did not consider the inclination of the side walls. Sitkei calculated the compression stress with respect to the position in the chamber considering one inclined side wall [3].

However, many assumptions were made here and average values were selected. Thus, this model is only suited for evaluating mean effects. More recently, Afzalinia and Roberge derived the stress-deformation relation in the compression chamber of a large square baler through a static-mechanical analysis [4]. Both inclined side walls and the roof were taken into account, but they reported that the model was only applicable at large compression pressures and that the inclination of the walls was approximated by an average value.

Because previous research only calculated the stresses along the chamber length, this research aims to calculate the deformations along the length of the compression chamber. This will allow for characterizing the compression and calculating the final bale density.

2. Methods

The stresses in the compression chamber are modeled in a similar way as described by Afzalinia and Roberge [4]. After deriving the force balances, the deformation along the chamber length will be calculated and compared to the measurements.

2.1. Modeling pressure and deformation along the depth of the chamber

List of abbreviations	
E, v	Young modulus [Pa] and Poisson coefficient [-]
h_x	Height of the compression chamber with the position x in the chamber [m]
h_0, b_0	Initial height and width of the chamber [m]
b_x	Width of the compression chamber with x [m]
ρ_0, ρ	Initial and actual density [kg/m³]
σ	Stress [Pa]
$\theta_{l,r,t}$	Inclination of the left and right side wall and of the roof [rad]
μ	Friction coefficient [-]

This study focuses on the compression of the crop while assuming a stationary condition, i.e. before the bale starts moving. For calculating the stress decay, the material is discretized in slices. The compression stresses of a slice are illustrated in Figure 1. The considered forces consist of the normal and friction forces on every side of the slice. In the compression direction, only the normal force is considered. The friction forces in Figure 1 are defined through Coulombs law of friction, with friction coefficient μ.

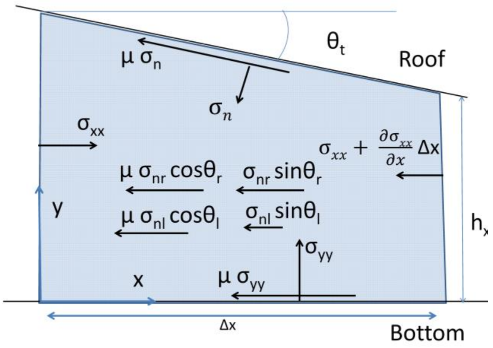

Figure 1 Stresses acting on the elementary volume, in the xy-plane

For small inclinations of the side walls and the roof, the following approximations can be made: $\theta_l = \theta_r$ and $\sin \theta_l = \theta_l$, $\cos \theta_l = 1$. This leads to the following force balances in *x, y* and *z*:

$$-\frac{\delta\, \sigma_{xx}}{\delta\, x} h_x b_x - \mu\, \sigma_{yy} b_x - \sigma_n(\mu + \theta_t) b_x - \sigma_{nl}(\theta_l + \mu) h_x - \sigma_{nr}(\theta_l + \mu) h_x = 0 \qquad (1)$$

$$\sigma_{yy} - \sigma_n(1 - \mu\theta_t) = 0 \qquad (2)$$

$$(\sigma_{nl} - \sigma_{nr})(\mu\theta_l - 1) h_x = 0 \qquad (3)$$

By entering the balances in *y* and *z* in the balance in *x*, the following relation is obtained:

$$\frac{\delta\sigma_{xx}}{\delta x} h_x b_x + \sigma_n b_x (2\mu - \mu^2\theta_t + \theta_t) + 2\sigma_{nl}(\theta_l + \mu) h_x = 0 \qquad (4)$$

Now, the stresses have to be linked with the deformation of the material. For this purpose, the material is assumed to be linear elastic and isotropic. This is implemented by using Hooke's general law:

$$\begin{bmatrix} \sigma_x \\ \sigma_y \\ \sigma_z \end{bmatrix} = \frac{E}{(1-2\nu)(1+\nu)} \begin{bmatrix} 1-\nu & \nu & \nu \\ \nu & 1-\nu & \nu \\ \nu & \nu & 1-\nu \end{bmatrix} \begin{bmatrix} \epsilon_x \\ \epsilon_y \\ \epsilon_z \end{bmatrix} \qquad (5)$$

With *E* Young's modulus and *v* the Poisson coefficient. The engineering strains (ϵ_y, ϵ_z) are written as a function of the height and width of the chamber as:

$$\epsilon_y = ln(h_x) - ln(h_0)$$

$$\epsilon_z = ln(b_x) - ln(b_0)$$

The assumption of small inclinations of side walls and roof gives the height and width of the chamber as: $h_x = h_0 - x\,\theta_t$ and $b_x = b_0 - 2\,\theta_l$. With these relations, Eq. (4) can be rewritten as:

$$h_x b_x (1-\nu)\ \frac{d\epsilon_x}{dx} = C + (A(1-\nu) + B\nu)\epsilon_y + \big(A\nu + B(1-\nu)\big)\epsilon_z + (A+B)\nu\epsilon_x \qquad (6)$$

Where

$$A = b_x(2\mu - \mu^2\theta_t + \theta_t)$$

$B = 2(\theta_l + \mu)h_x$

$C = \nu(\theta_t b_x + 2\,\theta_l h_x)$

This equation is solved by assuming the movement at the end of the fit to be 0, i.e. only the deformation is fitted and the clamped part is not considered.

2.2. Fitting the compression profile

The bale movement in the compression chamber of a large square baler was measured during baling of wheat straw. The measured compression profiles were then fitted with Eq. (6). The fitting algorithm minimized the sum of the squared errors between the model and the measured data by means of the interior-point method. The fitting was done using the non-linear, constrained optimization (fmincon) in MATLAB©.

The linear elastic material model (Eq. (6)) requires the Poisson coefficient *v*, the friction coefficient μ and an initial condition ϵ_0 for solving the differential equation. While *v* and μ have to be determined by the model fit, ϵ_0 can also be calculated. This can be done by using the linear elastic material model near the plunger, i.e. by taking Eq. (5) for σ_x with zero inclination of the side walls and the roof ($\epsilon_y = \epsilon_z = 0$). This approach requires the Young modulus to be determined by the fit and the stress on the plunger to be measured. Because the fit is sensitive to the initial condition and because of the inaccuracies of calculating it, the initial condition was also determined by the fit.

During compression by the plunger, more and more material will be deformed. At a certain plunger force, an extra deformation will move the bale instead of deforming more material. Hence, the deformation profile will not continue until the end of the compression chamber. Because the model assumes a stationary condition, only the significant (positive) deformations are considered when fitting the model and the remaining, stationary part of the bale will be left out.

3. Results

For representing the cost function, the initial condition is approximately calculated as described above. In Figure 3 the logarithm of this function at the estimated initial condition is given. The figure shows the fitting performance of the model as a function of μ and *v*. A slight dependency between both coefficients has to be noted. Near the absolute minimum, the cost function also shows several local minima which may cause the optimization to stop at non-realistic parameter sets.

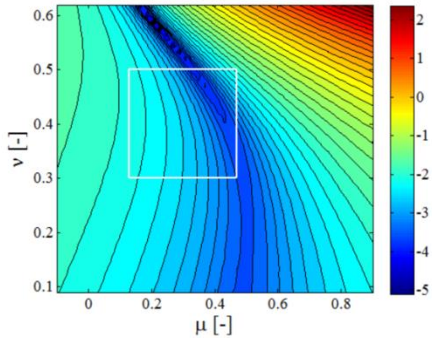

Figure 2 Logarithm of the cost function at the estimated initial condition for the linear elastic material model. The white rectangle indicates the expected region of the parameters.

In order to obtain feasible parameter sets, the optimization was started from multiple initial guesses inside the feasible parameter domain. To obtain a good distribution of the initial guesses over this domain a latin hypercube design was used. The parameter set with the smallest value for the cost function was then used as a solution. The resulting fit is shown in Figure 3. The position of zero deformation is only approximately known but the measurements show it should be between 1.4 and 1.9m in Figure 3. Extrapolating the model also shows the point of zero deformation to be in this region. The fit shows that the linear material model can capture the initial steep descend in the deformation, but an unexpected flexure point can be seen near the end of the deformation profile (1.5m in Figure 3). This does not seem feasible and might be due to the extrapolation beyond the last measurement point included in the parameter estimation.

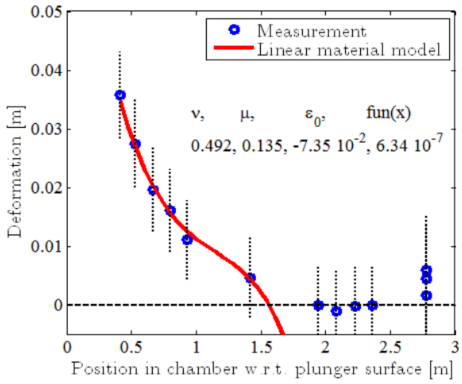

Figure 3 Fit of the deformation in the compression chamber with the linear elastic material model

4. Discussion

The straw used in this study approximately had a moisture content of 10%wb. The Poisson and friction coefficients reported in [4] are respectively 0.38 and 0.43 for wheat straw and 0.40 and 0.45 for barley straw. However, these values were measured at higher moisture contents, which could explain the rather large difference with the values in this study. Afzalinia & Roberge reported that the friction coefficient decreased with decreasing moisture content and was measured to be 0.15 at 12%w.b [5]. So, the estimated value of 0.135 is in agreement with their findings.

The current detection of the point of zero compression is based on the measurements. This detection is not accurate enough for proper model fitting.

It was indicated by Afzalinia and Roberge that the linear approximation of the constitutive material behaviour is only valid in a narrow pressure range. They reported that for high operating pressures this range suffices for describing the compression in a large square baler [4]. Expanding this range would require adjusting the parameters during compression. However, it might be more beneficial to use a non-linear model.

5. Conclusions

A linear crop compression model was elaborated to describe the force-deformation relation of a large square baler. By fitting the simulated deformation profiles to profiles measured in the bale chamber of a large square baler realistic values for the friction and Poisson coefficient of the compressed material were obtained. However, the current optimization knows influence from measurement error. Therefore, the parameter estimation and the calculation of the point of zero deformation should be improved.

References

[1] A. Ferrero, J. Horabik, and M. Molenda, “Density-pressure relationships in compaction of straw”, Canadian Agricultural Engineering, vol. 33 (1), (1990), pp. 107-111

[2] M. Faborode and J. O’Callaghan, “Theoretical analysis of the compression of fibrous agricultural materials”, Journal of Agricultural Engineering Research, vol. 35, (1986), pp. 175-191

[3] G. Sitkei, Mechanics of agricultural materials, Elsevier, Amsterdam, 1986

[4] S. Afzalinia and M. Roberge, “Modeling of pressure distribution inside the compression chamber of a large square baler”, in Transactions of the ASABE, Annual meeting of the American-Society-of-Agricultural-and-Biological-Engineers, vol.51, (2008), pp. 1143-1152

[5] S. Afzalinia and M. Roberge, “Physical and mechanical properties of selected forage materials”, Canadian Biosystems Engineering, vol. 49 (2007), pp. 2.23-2.27